

Conditional pair distributions in many-body systems: Exact results for Poisson ensembles

René D. Rohrmann*

*Instituto de Ciencias Astronómicas, de la Tierra y del Espacio,
UNSJ-CONICET, Av. España 1512 Sur, 5400 San Juan, Argentina*

Ernesto Zurbriggen†

Observatorio Astronómico, Universidad Nacional de Córdoba, Laprida 854, 5000 Córdoba, Argentina

(Dated: February 28, 2022)

We introduce a conditional pair distribution function (CPDF) which characterizes the probability density of finding an object (e.g., a particle in a fluid) to certain distance of other, with each of these two having a nearest neighbor to a fixed but otherwise arbitrary distance. This function describes special four-body configurations, but also contains contributions due to the so-called mutual nearest neighbor (two-body) and shared neighbor (three-body) configurations. The CPDF is introduced to improve a Helmholtz free energy method based on space partitions. We derive exact expressions of the CPDF and various associated quantities for randomly distributed, non-interacting points at Euclidean spaces of one, two and three dimensions. Results may be of interest in many diverse scientific fields, from fluid physics to social and biological sciences.

PACS numbers: 02.50.-r, 05.20.Jj, 51.30.+i

I. INTRODUCTION

Spatial distributions of objects are ubiquitous in nature. The pattern of distribution of a population can be characterized by statistical relationships between each component and its nearby companions. Methods based on neighbor relationships and two-point correlations are some of the simplest and most popular techniques for statistical pattern recognition. The analysis of spatial patterns is especially useful in modeling and describing a wide variety of natural [1–8] and social phenomena [9–13].

Methods for spatial structure studies of many-body systems have been developed and extensively applied in physics of condensed matter [14, 15]. Similar techniques are employed to understand the associations of galaxies and the large scale structures of the Universe [16, 17]. The main spatial structure function in the study of liquids is the pair distribution function (PDF). For statistically homogeneous and isotropic systems, which are the focus of this paper, the PDF is a radial function $g(r)$, translationally invariant, which characterizes the probability density of finding a particle at some given distance r from a reference particle. Assuming pairwise particle interactions, $g(r)$ can be used to obtain equations involving macroscopic thermodynamic variables [15]. An additional description can be obtained from k th-nearest-neighbor PDFs $g_k(r)$ [18–22]. The first nearest neighbor distribution, $g_1(r)$, is particularly useful to understand local fields around a particle in a fluid [23–26], or a star

in a stellar cluster or galaxy [27], and it has applications in other problems in physics [28]. However, a further detailed microscopic information is sometimes required to statistically characterize physical properties of fluids and materials. For instance, mutual-nearest-neighbor (MNN) pair descriptors are used in the study of solute relaxation processes in fluids [29], phonon spectra analysis of disordered systems [30], and for explaining the behavior of glass-forming liquids [31]. In general, the probability that particles in a fluid form MNN pairs can not be exactly deduced from the standard $g(r)$ or individual PDFs $g_k(r)$. Therefore, a superior spatial structure descriptor is highly desirable.

We propose here the introduction of a more complete description of the microscopic neighborhood structure around a reference particle. We introduce a conditional pair distribution function (CPDF) which gives the probability density of finding a particle to a certain distance from other in a fluid, with each of these two having a nearest neighbor to a fixed but otherwise arbitrary distance. This function describes special four-body configurations, but also contains contributions due to the mutual nearest neighbor (two-body) and shared neighbor (three-body) configurations. The new PDF is a spatial descriptor at the two-point distribution level but contains nontrivial higher-order structural information. In particular, it is a superior descriptor sensitive to topological connectedness information of the point pattern and could resolve a variety of degenerate point configurations associated with the standard PDF $g(r)$ [32].

The primary purpose of introducing the CPDF is to establish a correct expression for evaluating the interparticle potential energy in the so-called thermostistical space partition (TSP) formalism for fluids. The TSP approach, which was introduced in Ref. [33] for the case of pure substances and extended to mixtures in Ref. [34],

*Electronic address: rohr@icate-conicet.gob.ar;
URL: <http://icate-conicet.gob.ar/rohrmann>

†Electronic address: ernesto@oac.uncor.edu

was motivated by difficulties with the calculation and qualitative prediction of optical properties in white dwarf stars, currently based on the occupation probability formalism of Hummer & Mihalas [35] and whose consistency has been discussed in Ref. [36]. The TSP method combines the free-energy minimization technique [37] with space partitions that assign to each particle a volume v , which is determined by the distance of the particle to its closest neighbor, and roughly measures the free space surrounding each particle. The CPDF introduced in the present paper, denoted $g_{vv'}(r)$, is a PDF where the volumes v and v' of both pair particles are specified. It will be shown here that this CPDF is needed for an appropriate representation of the potential energy of fluids within the TSP formalism.

Explicit evaluation of the CPDF $g_{vv'}(r)$ is considerably more complicated than the computation of the conventional PDF $g(r)$. In the pairwise additive assumption for the potential energy of a fluid, the CPDF can be evaluated using a hierarchy of integral equations for s -body correlation functions, for instance the Yvon-Born-Green hierarchy [15], truncated by introducing some appropriate closure approximation. In the general case, with $g_{vv'}(r)$ representing four-particle configurations, the hierarchy expansion can be truncated in factors with correlation functions higher than $s = 5$ (in analogy with the mean-field approximation used in Ref. [29] to assess the MNN pair distribution of Lennard-Jones fluids). A method of calculating $g_{vv'}(r)$ by means of this scheme is currently being prepared in detail. In the present contribution we will restrict ourselves to the evaluation of $g_{vv'}(r)$ for random, non-interacting systems or so-called Poisson ensembles, which can be directly derived from simple and well-known probabilistic properties (e.g., [2, 38, 39]). The aim is two-fold. First, the study of the CPDF for random points may prove to be a useful guide for investigating this function in other systems, apart from its own importance at a fundamental level. Second, Poisson statistics is an especially powerful tool for studies of a wide variety of systems, and its CPDF may provide a new method of analysis. In fact, Poisson statistics emerges as a useful alternative in view of the practical limitations of a rigorous treatment for the complex natural systems. Random samples are employed very widely by comparison or contrast in the analysis of observed event data [40], or as a convenient first approximation to describe the spatial distribution of a variety of natural systems, from biological species [1–8] to stars on the sky [41–43]. The present work is part of an effort dedicated to improving the TSP formalism and to providing a well defined and very demanding test model of the CPDF for further research.

The paper is structured as follows. In Section II the conditional pair distribution function is formulated and general results are presented. Its implication within the TSP formalism is described in Section III. Section IV contains a derivation of the CPDF for Poisson patterns in one, two, and three spatial dimensions. Some derived results are examined there. Concluding remarks are con-

tained in Section VI.

II. DEFINITIONS AND GENERAL RELATIONS

Consider a system of N identical particles distributed in a D -dimensional Euclidean space with volume V . For conciseness, the radial distance r from a reference particle will be expressed in terms of the volume $\omega = \alpha r^D$ of a D -dimensional sphere of radius r centered in the particle, with

$$\alpha \equiv \frac{\pi^{D/2}}{\Gamma(1 + \frac{D}{2})}, \quad (2.1)$$

where Γ is the gamma function. The conventional PDF, henceforth expressed as $g(\omega)$, describes the probability density of finding a particle on the surface of a sphere of volume ω centered in the reference particle. More exactly, $g(\omega)$ is defined such that

$$ng(\omega)d\omega \equiv \text{mean number of particles between the surfaces of } \omega \text{ and } \omega + d\omega \text{ centered at the reference particle,} \quad (2.2)$$

where $n = N/V$ is the mean density in the fluid.

It is assumed here that for any reference particle there is one and only one nearest neighbor. This means that if two or more particles are equidistant from the reference, one of them will be arbitrarily designated as the first neighbor. The distance a between a particle and its nearest neighbor will be expressed by the volume v of a D -dimensional sphere of radius a . The volume v will be referred to as the *available volume* (AV) of the particle because it roughly measures the free-particle space surrounding it. The size distribution of AV in the fluid is given by the distribution n_v , where $n_v dv$ is the number density of particles with available volume between v and $v + dv$. The quantity $(n_v/n)dv$ is clearly the probability that the nearest neighbor lies in the volume dv of a spherical shell centered in the reference particle. Therefore, n_v/n is equivalent to the so-called *first neighbor distribution* [24–26]. In the thermodynamic limit ($N, V \rightarrow \infty$, keeping N/V constant), it follows that

$$n = \int_0^\infty n_v dv. \quad (2.3)$$

The conditional pair distribution functions $g_v(\omega)$ and $g_{vv'}(\omega)$ are defined by the following quantities

$$ng_v(\omega)d\omega \equiv \text{mean number of particles between the surfaces of } \omega \text{ and } \omega + d\omega \text{ centered at the reference particle with AV } v, \quad (2.4)$$

$$n_{v'}g_{vv'}(\omega)dv'd\omega \equiv \text{mean number of particles with AV between } v' \text{ and } v' + dv' \text{ lying between the spherical volumes } \omega \text{ and } \omega + d\omega \text{ centered at a particle with AV } v.$$

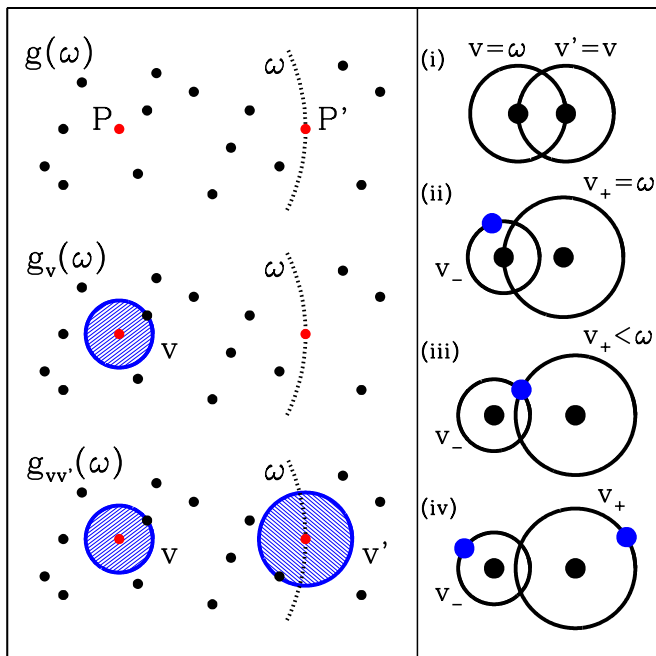


FIG. 1: (Color online) *Left*: Example of a point pattern with a characterization of the evaluation of the pair distribution functions $g(\omega)$, $g_v(\omega)$ and $g_{vv'}(\omega)$. The point P' lies in the surface of the spherical volume ω centered at the reference point P . Nearest neighbors of P and P' lie in the surfaces of spherical volumes v and v' centered in P and P' , respectively. *Right*: Representation of the four classes of (v, v') pairs (see text). Here, $v_+ \equiv \max(v, v')$ and $v_- \equiv \min(v, v')$.

(2.5)

According to the meaning of n_v , it is clear that $g(\omega)$ is just a weighted average of $g_v(\omega)$ over the whole range of v , that is

$$ng(\omega) = \int_0^\infty n_v g_v(\omega) dv. \quad (2.6)$$

Similarly, the integration of (2.5) over v' covering the whole range of available volume gives (2.4), i.e.,

$$ng_v(\omega) = \int_0^\infty n_{v'} g_{vv'}(\omega) dv'. \quad (2.7)$$

From (2.6) and (2.7) it follows that

$$n^2 g(\omega) = \int_0^\infty \int_0^\infty n_v n_{v'} g_{vv'}(\omega) dv dv'. \quad (2.8)$$

From the definitions given above, we can see that the function $g_v(\omega)$ is the probability density that a particle lies at the surface of a spherical volume ω centered in a randomly chosen particle *with* AV v . Similarly, $g_{vv'}(\omega)$ is the probability density of finding a particle with AV v' in the surface of a spherical volume ω centered in a particle with AV v . The conditional character of the probability

TABLE I: Classes of pairs (v, v') and some properties.

Configuration	n-body	ω -range
(i) mutual nearest neighbor	2	$\omega = v = v'$
(ii) simple nearest neighbor	3	$\omega = v_+ \equiv \max(v, v')$
(iii) shared nearest neighbor	3	$v_+ < \omega < \omega_{vv'}$
(iv) other	4	$v_+ < \omega$

densities $g_v(\omega)$ and $g_{vv'}(\omega)$ appear due to the specification of the AV v and v' for one or both particles of each pair. Due to the symmetry of the problem, the function $g_{vv'}(\omega)$ is symmetric in the variables v and v' . Fig. 1 (*left*) displays a schematic point pattern with characterizations of the standard PDF $g(\omega)$ and the CPDFs $g_v(\omega)$ and $g_{vv'}(\omega)$. The function $g_{vv'}(\omega)$ and the distribution n_v are the central quantities of the present issue since knowledge of them allows one to calculate $g_v(\omega)$ and $g(\omega)$ with (2.7) and (2.8).

The function $g_{vv'}(\omega)$ describes in general four-body configurations, i.e., pairs (v, v') composed of two particles with a third particle in the surface of the volume v centered in the first one and a fourth particle in the surface of v' centered in the second one. However, there are also other configurations of pairs (v, v') formed by only two or three particles. As is illustrated in Fig. 1 (*right*) and detailed in Table I, there are four independent classes of pairs (v, v') :

- *Class (i)* denotes mutual nearest neighbors, i.e., each particle of the pair (v, v') is the nearest neighbor of the other.
- *Class (ii)* corresponds to the configuration where one and only one particle of the pair (v, v') is the nearest neighbor of the other.
- *Class (iii)* refers to the shared nearest neighbor configuration, i.e., both particles of the pair (v, v') have the same nearest neighbor.
- *Class (iv)* denotes pairs (v, v') which involve a configuration with four different particles.

Because classes (i-iv) are mutually exclusive and exhaustive, we have

$$g_{vv'}(\omega) = g_{vv'}^{(i)}(\omega) + g_{vv'}^{(ii)}(\omega) + g_{vv'}^{(iii)}(\omega) + g_{vv'}^{(iv)}(\omega), \quad (2.9)$$

where $g_{vv'}^{(\nu)}(\omega)$ is the contribution to $g_{vv'}(\omega)$ due to pairs (v, v') of class (ν) .

Geometrical considerations which involves the available volume v of a particle or, equally, the distance to its nearest neighbor, can be employed to derive some general properties of the contributions to $g_{vv'}(\omega)$ on the right hand side of (2.9). As can be seen from Fig. 1, pairs class (i) only occurs for $\omega = v = v'$ and, therefore, the mathematical representation of the term $g_{vv'}^{(i)}(\omega)$ must have singularities. Indeed, taking into account (2.5), it is easily demonstrated that this term is proportional to the

product of two Dirac delta functions,

$$g_{vv'}^{(i)}(\omega) \propto \delta(v - v')\delta(\omega - v). \quad (2.10)$$

A similar behavior is deduced for the second term on the right-hand side of (2.9). Pairs (v, v') of class (ii) occur only for $\omega = v_+$, with

$$v_+ \equiv \max(v, v'), \quad (2.11)$$

and therefore

$$g_{vv'}^{(ii)}(\omega) \propto \delta(\omega - v_+). \quad (2.12)$$

Since two particles cannot share the nearest neighbor when their volumes v and v' do not overlap, the third term on the right of (2.9) vanishes for $\omega > \omega_{vv'}$, where

$$\omega_{vv'} \equiv (v^{1/D} + v'^{1/D})^D. \quad (2.13)$$

The third term vanishes also at $\omega < v_+$ because no particle lies at lower distance than the nearest neighbor. Thus

$$g_{vv'}^{(iii)}(\omega) = 0, \quad \omega \notin (v_+, \omega_{vv'}). \quad (2.14)$$

Similarly, the fourth term vanishes for $\omega < v_+$,

$$g_{vv'}^{(iv)}(\omega) = 0, \quad \omega < v_+. \quad (2.15)$$

Therefore, $g_{vv'}(\omega)$ vanishes at $\omega < v_+$ and has singularities for pair configurations with $\omega = v = v'$ and $\omega = v_+$.

At the fluid context and in analogy to the standard PDF, one may expect that, at sufficiently large interparticle distances (large ω), pairs (v, v') are uncorrelated and the CPDF must then reduce to unity

$$\lim_{\omega \rightarrow \infty} g_{vv'}(\omega) = 1. \quad (2.16)$$

III. THE ROLE PLAYED BY $g_{vv'}(\omega)$ IN THE TSP FORMALISM

Let us define $u_{vv'}(\omega)$ as the interparticle potential between two particles forming a pair (v, v') , with a particle centered in the volume ω and another one located on the surface of ω . The potential $u_{vv'}(\omega)$, where the AV v and v' for both pair particle are specified, is a generalization of the usual pairwise interparticle potential $u(\omega)$. $u_{vv'}(\omega)$ formally takes into account perturbative effects on the two-body interaction potential introduced by the nearest neighbor of each particle in the pair. Many-body contributions to effective pair potentials are known for liquid hydrogen [44–46] and have been theoretically considered for fluid helium [47]. However, potential energy surfaces of four-particle systems are needed for a full knowledge of $u_{vv'}(\omega)$ in a fluid. For the moment, *ab initio* potential evaluations are limited to three-body systems at few geometrical configurations and for some atomic, molecular and colloidal systems [48–50].

Multiplication of (2.5) with $u_{vv'}(\omega)$ and integration over all ω , v and v' , yields the total potential energy of the system

$$\Phi = \frac{1}{2V} \int_0^V \int_0^V N_v N_{v'} \left[\int u_{vv'}(\omega) g_{vv'}(\omega) d\omega \right] dv' dv, \quad (3.1)$$

where $N_v = n_v V$, $N_{v'} = n_{v'} V$, and the factor 1/2 avoids the double count of pairs (v, v') . If one writes

$$u_v(\omega) = \frac{\int n_{v'} u_{vv'}(\omega) g_{vv'}(\omega) dv'}{\int n_{v'} g_{vv'}(\omega) dv'}, \quad (3.2)$$

then (3.1) can alternatively be written as

$$\Phi = \frac{N}{2V} \int_0^V N_v \left[\int u_v(\omega) g_v(\omega) d\omega \right] dv. \quad (3.3)$$

Similarly, if we define an averaged pair potential as

$$u(\omega) = \frac{\int n_v u_v(\omega) g_v(\omega) dv}{\int n_v g_v(\omega) dv}, \quad (3.4)$$

then the total potential expression reduces to that typically used in physics of liquids, which is based on the conventional PDF $g(\omega)$, i.e.,

$$\Phi = \frac{N^2}{2V} \int u(\omega) g(\omega) d\omega. \quad (3.5)$$

For systems with two-particle potential without many-body effects, $u_{vv'}(\omega) = u_v(\omega) = u(\omega)$. Otherwise, the CPDF $g_{vv'}(\omega)$ can be used to calculate *effective* pair potentials [Eqs. (3.2) and (3.4)] directly from *ab initio* many-body potentials $u_{vv'}(\omega)$ (when these become available), and thus the conventional evaluation of the total potential energy in liquid theory is preserved [Eq. (3.5)].

The thermostatical space partition (TSP) formalism is a mathematical model for moderately dilute gases which combines the free-energy minimization method [37] with space partitions. It was developed for one-component [33] and multi-component [34] fluids. Applications to simple gas models (hard spheres, van der Waals fluids, attractive particles, and partially ionized hydrogen gas) have shown that TSP provides a useful tool to evaluate self-consistently thermodynamic and structural properties of gases at low densities as found in white dwarf atmospheres, where conventional techniques fail to reproduce gas opacities affected by non-ideal effects (e.g., the Lyman continuum opacity [36, 51]). The novel feature of the TSP formalism is that it allows one to evaluate, in a thermodynamically self-consistent way, populations of atoms and molecules in internal energy states as a function of the available volume v , a variable linked directly with different degrees of interparticle perturbation.

For one-component fluids, the TSP formalism is defined in terms of a Helmholtz free-energy model A based on the occupation number distribution N_v of the variable v [33],

$$A = \int_0^V \frac{N_v}{\beta} \ln \left(\frac{N_v \lambda^D}{N} \right) dv + \Phi, \quad (3.6)$$

where $\beta = 1/(kT)$, $\lambda = \sqrt{h^2\beta/(2\pi m)}$, D is the space dimension, k the Boltzmann constant, h the Planck constant, m the particle mass and T the temperature. The first term on the right hand side of Eq. (3.6) is the ideal free energy as given by the TSP formalism. The space distribution N_v for a particle system at equilibrium is determined by minimization of A subjected to total particle number and total volume constrains (see [33] for details),

$$N = \int_0^V N_v dv, \quad (3.7)$$

$$V = \int_0^V v N_v dv. \quad (3.8)$$

In Ref. [33], the interparticle interactions in the fluid were incorporated into the TSP approach via the potential $u_v(\omega)$ and the PDF $g_v(\omega)$. Therefore, the total potential energy Φ was written in [33] as (3.3), but assuming that $u_v(\omega)$ is *independent* of N_v . In such case, Φ is a *linear* functional of N_v and the minimization free energy procedure yields

$$N_v = \frac{N}{\lambda^D} \exp \left[-\beta \left(\gamma v + \frac{\phi_v}{2} + \frac{\Phi}{N} - \mu \right) \right], \quad (3.9)$$

with

$$\phi_v = n \int u_v(\omega) g_v(\omega) d\omega \quad (3.10)$$

where μ , the chemical potential, and $\gamma = P - \Phi/V$, the pressure minus the potential energy density, are the Lagrange multipliers for our constrains.

However, if we adopt the more general potential energy expression given by (3.1), Φ is a *quadratic* functional of N_v . In this case, it is easily deduced that the minimization technique leads to

$$N_v = \frac{N}{\lambda^D} \exp [-\beta(\gamma v + \phi_v - \mu)], \quad (3.11)$$

with ϕ_v and $u_v(\omega)$ respectively given by (3.10) and (3.2) or, equivalently,

$$\phi_v = \int \int n_{v'} u_{vv'}(\omega) g_{vv'}(\omega) dv' d\omega. \quad (3.12)$$

The main difference between Eqs. (3.9) and (3.11) is the dependence of N_v on ϕ_v . It is important to note that the results obtained in [33] from the TSP approach for hard systems and van der Waals fluids remain unchanged if one uses (3.11) instead (3.9). This is because of the special form of the two-particle potentials for these systems. However, Eq. (3.11) is the correct one and must be used in general. In particular, Eq. (3.11) is supported by results corresponding to attractive hard spheres (AHS). The implementation of the TSP approach to the AHS model

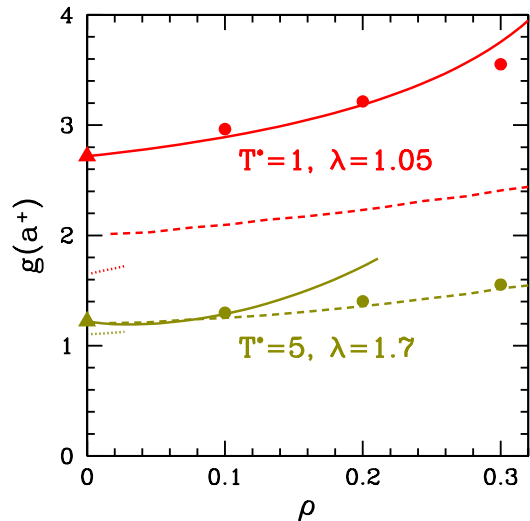


FIG. 2: (Color online) Contact values $g(a^+)$ of the PDF for attractive hard spheres in the TSP formalism based on Eq. (3.11) (solid lines), are compared with exact values in the limit of zero density (triangles), Monte Carlo simulations [52] (circles), results of a perturbative theory [53] (dashed lines), and results derived from Eq. (3.9) (dotted lines). Here $T^* = kT/\epsilon$ is the reduced temperature, $\rho = nd^3$ the reduced number density, and λ the potential range in units of the particle diameter d [i.e., $\xi = a(\lambda^3 - 1)$ and $a = 4\pi d^3/3$ in Eq. (D1)].

is shown in Appendix D. We obtain the following contact value of the conventional PDF for this model,

$$g(\omega = a^+) = \frac{\beta\gamma}{nB} e^{\beta\epsilon(1+n\xi)}, \quad (3.13)$$

with $\beta\gamma$ and B given by Eqs. (D5) and (D6). A density expansion of (3.13) yields

$$g(a^+) = e^{\beta\epsilon} \{ 1 + [b + (2 + \beta\epsilon - 2e^{\beta\epsilon})\xi] n + O(n^2) \}, \quad (3.14)$$

in agreement with the value expected at zero density $g(a^+) = e^{-\beta u(a^+)} = e^{\beta\epsilon}$. On the contrary, it may be deduced that the contact value at zero density resulting from Eq. (3.9) is incorrectly $e^{\beta\epsilon/2}$. Although the TSP approach is being developed mainly for the low densities found in stellar atmospheres, Fig. 2 shows that Eq. (3.13) can also reproduce satisfactorily the results at moderately low densities obtained from Monte Carlo simulations [52]. In conclusion, the correct expression (3.11) for the space distribution N_v at equilibrium in the TSP formalism, is reached with the minimization of a free energy model based on the quadratic functional (3.1) for the system potential energy and the use of the CPDF $g_{vv'}(\omega)$.

IV. POISSON ENSEMBLES

In this section we deduce an exact expression of $g_{vv'}(\omega)$ for an infinite system composed of independent and ran-

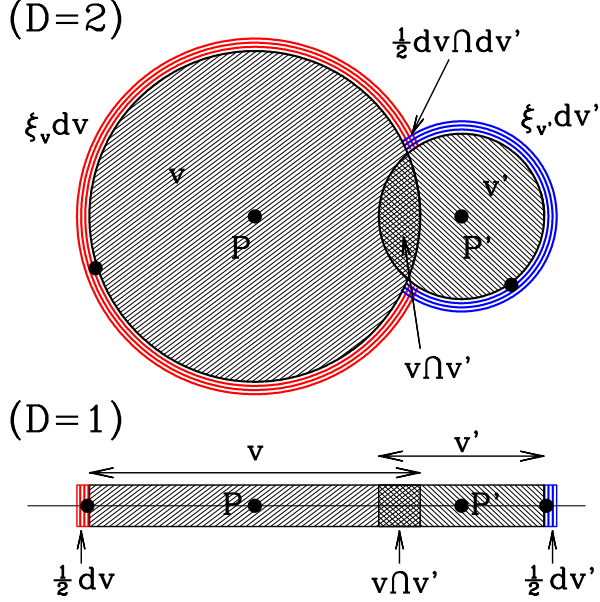


FIG. 3: (Color online) Pairs (v, v') showing various geometrical quantities involved in the evaluation of the CPDF $g_{vv'}(\omega)$ for Poisson ensembles in one and two dimensions.

domly distributed points, the so-called Poisson ensemble. This system is equivalent to the thermodynamic limit of a fluid with non-interacting particles (the perfect or ideal gas, sometimes called Poisson fluid in the mathematics literature). Poisson ensemble serves as a prototype of more general point systems.

The nearest neighbor distribution for random configurations of non-interacting points in three dimension was derived by Hertz [23]. In the present notation, the distribution n_v for Poisson ensembles in arbitrary dimension is given by

$$n_v = n^2 e^{-nv}. \quad (4.1)$$

This distribution can also be derived from the TSP method [33]. Indeed, (4.1) is the minimum Helmholtz energy solution [Eq. (3.11) with $\phi_v = 0$] for the distribution of available volume with the constrains of particle conservation (3.7) and space normalization (3.8) in the thermodynamic limit.

For the evaluation of $g_{vv'}(\omega)$, we use two basic properties which characterize to a Poisson point process in arbitrary dimension and with average density n :

(A) the probability that a given volume Ω is found empty of points, except by a prescribed and finite number of them, is $e^{-n\Omega}$, (4.2)

(B) the probability of finding a point within an infinitesimal volume $d\Omega$ is $nd\Omega$. (4.3)

We now apply these properties in the evaluation of the occurrence probability of pairs (v, v') in classes (i-iv). We

call δp the probability for the occurrence of a pair (v, v') with the second point (say P'), which has an AV between v' and $v' + \delta v'$, lying between the surfaces of volumes ω and $\omega + \delta\omega$ centered in the reference point (say P), which has an AV between v and $v + \delta v$. By definition of $g_{vv'}(\omega)$, Eq. (2.5), it is evident that the probability δp can be expressed as follows

$$\delta p = n^{-1} n_v n_{v'} g_{vv'}^{(v)}(\omega) \delta v \delta v' \delta \omega. \quad (4.4)$$

On the other hand, in the case of configurations class (iv) and according to (4.2) and (4.3), the probability δp equals the product of the following four probabilities (see Fig. 3):

(a) the probability $(n\delta\omega)$ that the point P' (P) lies between the surfaces of ω and $\omega + \delta\omega$ centered in P' (P),

(b) the probability $(n\xi_v \delta v)$ of finding a point between the surfaces of v and $v + \delta v$ centered at P , where ξ_v is the fraction of δv that is not shared with v' ,

$$\xi_v \equiv 1 - \frac{\delta v \cap v'}{\delta v}, \quad (4.5)$$

(c) the probability $(n\xi_{v'} \delta v')$ of finding a point between the surfaces of v' and $v' + \delta v'$ centered at P' , $\xi_{v'}$ being the fraction of $\delta v'$ that is not shared with v ,

$$\xi_{v'} \equiv 1 - \frac{\delta v' \cap v}{\delta v'}, \quad (4.6)$$

(d) the probability $(e^{-nv \cup v'})$ that no points, apart from P and P' , lie in the union volume $v \cup v'$.

For notational simplicity, explicit ω and v' (v) dependence has been omitted for ξ_v ($\xi_{v'}$). In (b) and (c) we have used the fact that, due to the meaning of available volume, there is no point into portions of δv and $\delta v'$ which overlap with v' and v , respectively. Thus, for pairs in class (iv) we obtain

$$\delta p = e^{-nv \cup v'} (n\xi_v \delta v) (n\xi_{v'} \delta v') (n\delta\omega) \Theta(\omega - v_+), \quad (4.7)$$

where $\Theta(x)$ is the usual Heaviside step function, which here takes into account that pair configurations with $\omega < \max\{v, v'\}$ are forbidden [Eq. (2.15)]. Therefore, using (4.1) and that $v \cup v' = v + v' - v \cap v'$, it follows from (4.4) and (4.7) that

$$g_{vv'}^{(iv)}(\omega) = \xi_v \xi_{v'} e^{nv \cap v'} \Theta(\omega - v_+). \quad (4.8)$$

A similar procedure applies immediately to pairs (v, v') in classes (i-iii). In the case (iii) we must replace the assumptions (b) and (c) by the probability $(n\delta v \cap \delta v')$ of finding the shared nearest neighbor inside of intersection volume $(\delta v \cap \delta v')$ of the spherical shells δv and $\delta v'$ surrounding P and P' , respectively (Fig. 4). Then

$$g_{vv'}^{(iii)}(\omega) = \frac{\eta_{vv'}}{n} e^{nv \cap v'} \Theta(\omega - v_+), \quad (4.9)$$

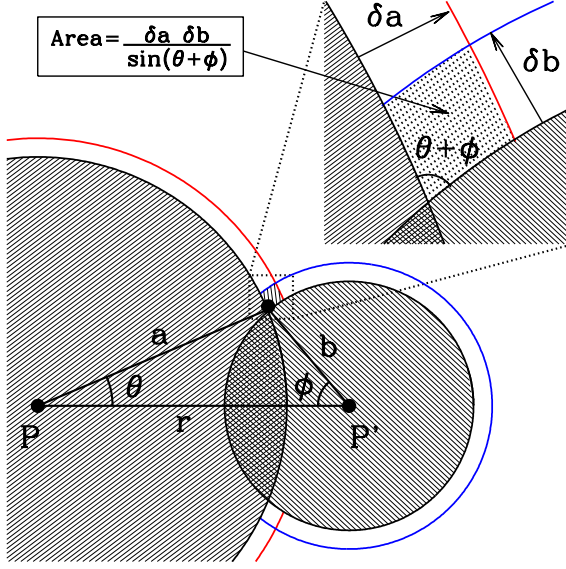


FIG. 4: (Color online) Shared neighbor configuration for $D \geq 2$.

where $\eta_{vv'}$ represents the ratio between the volume of intersection and the volume product of both shells,

$$\eta_{vv'} \equiv \frac{\delta v \cap \delta v'}{\delta v \delta v'} \quad (4.10)$$

(the ω dependence of $\eta_{vv'}$ is omitted for brevity). For pairs of class (i), i.e. mutual neighbors, the probabilities (b) and (c) are just considered by (a) and must be replaced by Dirac delta distributions as expressed by Eq. (2.10). Then

$$g_{vv'}^{(i)}(\omega) = \frac{1}{n^2} \delta(v - v') \delta(\omega - v) e^{n\zeta v}, \quad (4.11)$$

where ζ is the fraction of the overlap volume ($v \cap v'/v$) of two spheres with equivalent size and whose centers are separated by a distance equal to their radii (notice that ζ depends exclusively on the dimensionality D). Some ζ values are given in Table II below. Similarly, in the case of pairs of class (ii), the probability of finding a nearest neighbor as given by either (b) or (c) is just included in the probability (a) and, according to (2.12), we have

$$g_{vv'}^{(ii)}(\omega) = \frac{\xi_{v_-}}{n} \delta(\omega - v_+) e^{nv \cap v'}. \quad (4.12)$$

with

$$v_- \equiv \min(v, v'). \quad (4.13)$$

Substitution of expressions (4.8), (4.9), (4.12) and (4.11) into (2.9) yields the CPDF for Poisson ensembles

$$g_{vv'}(\omega) = e^{nv \cap v'} \left[\left(\frac{\delta(v - v')}{n^2} + \frac{\xi_{v_-}}{n} \right) \delta(\omega - v_+) \right.$$

$$\left. + \left(\frac{\eta_{vv'}}{n} + \xi_v \xi_{v'} \right) \Theta(\omega - v_+) \right]. \quad (4.14)$$

The cross-section $v \cap v'$ between v and v' for one-dimensional pairs (v, v') is easily deduced to be $(v + v' - \omega)/2$ at $\omega \leq v + v'$ and zero otherwise. Results for $D = 2$ and $D = 3$ can be also deduced by simple geometry. Specifically, one finds that [54]

$$v \cap v' = \begin{cases} \frac{1}{2}(v + v' - \omega), & (D = 1) \\ \frac{v}{\pi} \left[\theta - \frac{1}{2} \sin(2\theta) \right] \\ + \frac{v'}{\pi} \left[\phi - \frac{1}{2} \sin(2\phi) \right], & (D = 2) \\ \frac{v}{4} (2 - 3 \cos \theta + \cos^3 \theta) \\ + \frac{v'}{4} (2 - 3 \cos \phi + \cos^3 \phi), & (D = 3) \end{cases} \quad (4.15)$$

for $v_+ \leq \omega \leq \omega_{vv'}$ and $v \cap v' = 0$ for $\omega > \omega_{vv'}$, where the angles θ and ϕ are given by ($D \geq 2$)

$$\cos \theta = \frac{\omega^{2/D} + v^{2/D} - v'^{2/D}}{2(\omega v)^{1/D}}, \quad (4.16)$$

$$\cos \phi = \frac{\omega^{2/D} + v'^{2/D} - v^{2/D}}{2(\omega v')^{1/D}}. \quad (4.17)$$

The quantities $\xi_v, \xi_{v'}, \eta_{vv'}$ in (4.14) can be evaluated in terms of elementary functions. For $\omega > \omega_{vv'}$, with $\omega_{vv'}$ given by Eq. (2.13), we have $\xi_v = \xi_{v'} = 1, \eta_{vv'} = 0, v \cap v' = 0$, and therefore

$$g_{vv'}(\omega) = g_{vv'}^{(iv)}(\omega) = 1, \quad \omega > \omega_{vv'}. \quad (4.18)$$

For $v_+ \leq \omega \leq \omega_{vv'}$, it can be shown easily (with help of Figs. 3 and 4) that

$$\xi_v = \begin{cases} \frac{1}{2}, & (D = 1) \\ 1 - \theta/\pi, & (D = 2) \\ \frac{1}{2}(1 + \cos \theta), & (D = 3) \end{cases}, \quad \xi_{v'} = \begin{cases} \frac{1}{2}, & (D = 1) \\ 1 - \phi/\pi, & (D = 2) \\ \frac{1}{2}(1 + \cos \phi), & (D = 3) \end{cases} \quad (4.19)$$

and

$$\eta_{vv'} = \begin{cases} \frac{1}{2} \delta(\omega - v - v'), & (D = 1) \\ (2\pi \sqrt{vv'} \sin[\theta + \phi])^{-1}, & (D = 2) \\ \sin \theta [6v^{1/3} v'^{2/3} \sin(\theta + \phi)]^{-1}. & (D = 3) \end{cases} \quad (4.20)$$

Some guidelines for the derivation of $\eta_{vv'}$ are given in Appendix A. Although $\eta_{vv'}$ was written in a particular way for $D = 3$, it is actually symmetric with respect to v and v' . Notice also that the prefactor $1/2$ in (4.19) and (4.20) for $D = 1$ is related to the ‘‘edge surface’’ of the one-dimensional ‘‘volumes’’ v and v' (see Fig. 3).

A. Explicit expressions for $D = 1$ and $D \rightarrow \infty$

Substantial simplifications in Eq. (4.14) occur in the limits of one and infinitely many space dimensions. In particular, the combination of (4.14) with results (4.15),

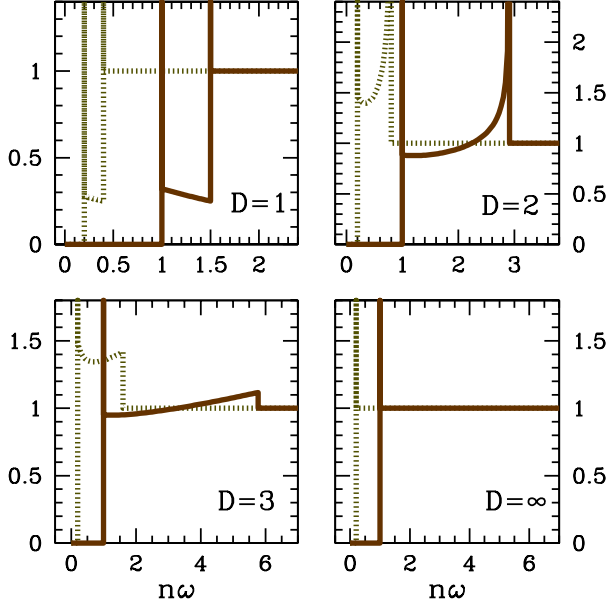


FIG. 5: (Color online) Evaluations of $g_{vv'}(\omega)$ at dimensions $D = 1, 2, 3, \infty$ for $(nv, nv') = (0.2, 0.2)$ (dotted lines) and $(nv, nv') = (1, 0.5)$ (solid lines).

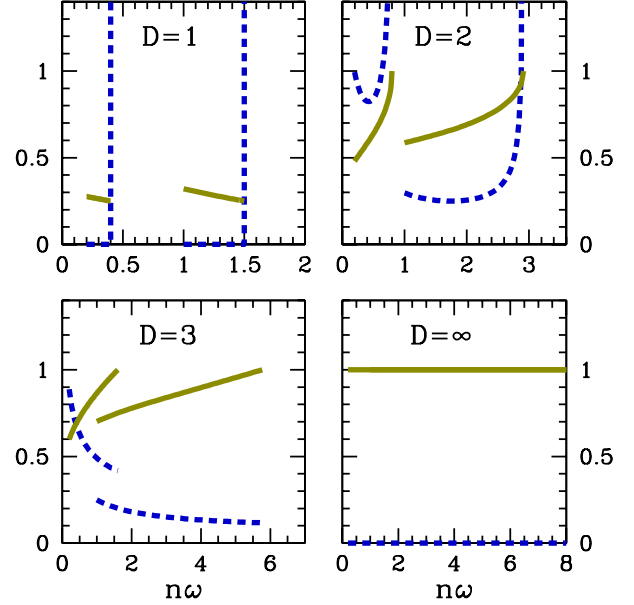


FIG. 6: (Color online) Contributions $g_{vv'}^{(iii)}(\omega)$ and $g^{(iv)}(\omega)$ (dashed and solid lines, respectively) to $g_{vv'}(\omega)$ at $v_+ < \omega < \omega_{vv'}$, for $D = 1, 2, 3, \infty$, and for the two (v, v') conditions shown in Fig. 5.

(4.19) and (4.20) at $D = 1$, gives the CPDF for one dimensional Poisson systems

$$\begin{aligned}
 g_{vv'}(\omega) = & \left[\frac{e^{(nv)/2}}{n^2} \delta(v - v') + \frac{e^{(nv_-)/2}}{2n} \right] \delta(\omega - v_+) \\
 & + \frac{e^{n(v+v'-\omega)/2}}{4} \Theta(v + v' - \omega) \Theta(\omega - v_+) \\
 & + \frac{1}{2n} \delta(\omega - v - v') + \Theta(\omega - v - v'). \quad (4.21)
 \end{aligned}$$

On the other hand, as the spatial dimension tends to infinite the intersection volume of two off-center hyperspheres ($v \cap v'$), the overlap space between two off-center hyperspherical shells ($\delta v \cap \delta v'$), and the cross section between a hyperspherical shell and a hypersphere ($\delta v \cap v'$) no centered, all go to zero. Consequently, $\xi_v = \xi_{v'} \rightarrow 1$ and $\eta_{vv'} \rightarrow 0$ everywhere as $D \rightarrow \infty$, and therefore (4.14) reduces to

$$g_{vv'}(\omega) = \left[\frac{1}{n^2} \delta(v - v') + \frac{1}{n} \right] \delta(\omega - v_+) + \Theta(\omega - v_+). \quad (4.22)$$

One of the main differences between the CPDF of Poisson ensembles at one and infinite space dimensions concerns the shared neighbor contribution. For $D = 1$, $g_{vv'}^{(iii)}(\omega)$ is a singular function that corresponds to a single point of contact between v and v' , while that at $D = \infty$ the probability density of finding a pair sharing the first neighbor tends to zero everywhere because $\eta_{vv'} \rightarrow 0$.

B. Discussion

In Fig. 5 we depict evaluations of $g_{vv'}(\omega)$ based on Eq. (4.14) for $D = 1, 2, 3$, and ∞ , at $(nv, nv') = (0.2, 0.2)$ and $(nv, nv') = (1, 0.5)$ (dotted and solid lines, respectively). For the same conditions, Fig. 6 shows the contributions to $g_{vv'}(\omega)$ originated by pairs (v, v') in classes (iii) and (iv), as given by Eqs. (4.9) and (4.8). The contribution which shows the largest variations is $g_{vv'}^{(iii)}(\omega)$, a direct consequence of the complex dependence of the overlap shell volume $\eta_{vv'}$ with the parameters v, v' and ω .

As observed in Fig. 5, $g_{vv'}(\omega)$ vanishes for all dimension at $\omega < v_+$, which means that there are not very close pairs (v, v') as a consequence of the exclusion zones imposed by the AV v and v' . The main striking features on the plots are the strong correlations between pairs (v, v') at $\omega = v_+$ for all dimensions and at $\omega = \omega_{vv'}$ for $D = 1$ and 2. For, respectively, $D = 1, 2$ and 3, $\omega_{vv'} = 0.4, 0.8$ and 1.6 in the case of pairs $(nv, nv') = (0.2, 0.2)$, and $\omega_{vv'} = 1.5, 2.914$ and 5.771 in the case $(nv, nv') = (1, 0.5)$.

The singularity at $\omega = v_+$, denoted by vertical lines in Fig. 5, is produced by pairs where at least one of the two points is the nearest neighbor of the other one, i.e., it has origin in pairs of type (ii), together with pairs of type (i) for the example with $v = v'$ (mutual nearest neighbors). The second strong correlation originated at one and two dimensions is due to the shared nearest neighbor configuration, i.e., pairs in class (iii). For $D = 1$, the singularity introduced by the $\delta(\omega - v - v')$ function in Eq. (4.21), seen as vertical lines in Fig. 6, is a consequence of the fact that

the shared neighbor must be located in the intersection of the outer edges of v and v' , which for $D = 1$ corresponds to a single point in space. In the case of two-dimensional Poisson ensembles, the scaled overlap volume $\eta_{vv'}$ gives nonzero values in the range $v_+ < \omega < \omega_{vv'}$ and has a singularity at $\omega = \omega_{vv'}$, which is reflected in a dramatic rise of $g_{vv'}(\omega)$ (Fig. 5, $D = 2$).

At $D = 3$, the overlapping $\eta_{vv'}$ of the outer edges of v and v' is less sensitive to variation of ω and therefore the contribution $g_{vv'}^{(iii)}(\omega)$ remains bounded for all ω (Fig. 6). In this dimension, the discontinuity in $g_{vv'}(\omega)$ at $\omega = \omega_{vv'}$ (Fig. 5) is yielded by the sudden fall of the occurrence of shared neighbor pairs. For $D = \infty$, the contribution of shared nearest neighbor configurations is everywhere negligible (dashed line in Fig. 6) and that from pairs of class (iv) is uniform and equals unity (solid line), the total CPDF resulting flat at $\omega > v_+$ (Fig. 5).

V. THE CPDF $g_v(\omega)$ AT POISSON ENSEMBLES

An expression for $g_v(\omega)$ corresponding to Poisson ensembles can be obtained in a similar, but simpler and more straightforward way than that previously used for $g_{vv'}(\omega)$ (its derivation is left to the reader). This CPDF was previously introduced and analyzed in [33] and reads

$$g_v(\omega) = \frac{1}{n} \delta(\omega - v) + \Theta(\omega - v). \quad (5.1)$$

Here, the Dirac delta function accounts for the nearest neighbor contribution of a reference point with AV v , and the Heaviside function describes the probability density of finding points (other than the nearest one) lying in the surface of $\omega > v$ centered in the reference one. It should be noted that (5.1) could be derived from (2.7) and (4.14), but this procedure involves some analytically intractable integrals for $D \geq 2$.

On the other hand, substitution of (5.1) into (2.6) provides the expected PDF for Poisson ensembles, i.e.,

$$g(\omega) = 1. \quad (5.2)$$

This result reflects the well-known fact that no correlation exists between pairs of arbitrary points at Poisson ensembles. Clearly the departures from unity in $g_v(\omega)$ and $g_{vv'}(\omega)$ are due to that the available volumes v and v' introduce correlations between pairs at short distances, which correspond to $\omega \leq v$ and $\omega \leq \omega_{vv'}$ for $g_v(\omega)$ and $g_{vv'}(\omega)$, respectively.

A. Relative importance of the different contributions to the CPDF $g_v(\omega)$

The results obtained in the derivation of $g_{vv'}(\omega)$ can be used to evaluate various statistical neighboring functions. In particular, expressions (2.6) and (2.7) can be applied

to each class ($\nu = \text{i, ii, iii, iv}$) of pairs (v, v') ,

$$g_v^{(\nu)}(\omega) = \frac{1}{n} \int_0^\infty n_{v'} g_{vv'}^{(\nu)}(\omega) dv', \quad (5.3)$$

$$g^{(\nu)}(\omega) = \frac{1}{n} \int_0^\infty n_v g_v^{(\nu)}(\omega) dv. \quad (5.4)$$

The quantities in Eqs. (5.3) and (5.4) express partial probability densities that describe the spatial distributions of specific pair configurations. For mutual neighbor pairs, from (4.11), (5.3), and (5.4) we obtain

$$g_v^{(i)}(\omega) = \frac{1}{n} e^{(\zeta-1)nv} \delta(\omega - v), \quad (5.5)$$

$$g^{(i)}(\omega) = e^{(\zeta-2)n\omega}. \quad (5.6)$$

Here, it is useful to separate pairs in class (ii) into subclasses (iia) and (iib). Pairs (v, v') where the point with AV v' is the (non mutual) nearest neighbor of the point with AV v belong to the subclass (iia), otherwise they belong to the subclass (iib). Then, Eq. (5.3) yields

$$g_v^{(ii)}(\omega) = g_v^{(iia)}(\omega) + g_v^{(iib)}(\omega) \quad (5.7)$$

with

$$g_v^{(iia)}(\omega) = \delta(\omega - v) \int_0^v \xi_{v'} e^{-nC_{v'}} dv', \quad (5.8)$$

and

$$g_v^{(iib)}(\omega) = [\xi_v e^{-nC_{v'}}]_{v'=\omega} \Theta(\omega - v), \quad (5.9)$$

where $C_{v'} = v' - v \cap v'$ is the volume of a crescent in the intersection of v and v' . The term $g_v^{(iia)}(\omega)$ is the probability density of finding a non-mutual, first neighbor in the surface of ω centered in a reference point with AV v . The term $g_v^{(iib)}(\omega)$ is the contribution to $g_v(\omega)$ due to pairs where the reference point with AV v is the non-mutual nearest neighbor of the other one. Note that the Dirac delta term in (5.1) arises from contributions due to $g_v^{(i)}(\omega)$ and $g_v^{(iia)}(\omega)$ through (2.7), which then implies that the integral in (5.8) is given by

$$\int_0^v \xi_{v'} e^{-nC_{v'}} dv' = \frac{1}{n} [1 - e^{(\zeta-1)nv}]. \quad (5.10)$$

The contribution to the PDF $g(\omega)$ due to pairs in subclasses (iia) and (iib) may be found from (5.4), (5.8) and (5.9). Thus, using (5.10), one obtains

$$g^{(iia)}(\omega) = e^{-n\omega} - e^{(\zeta-2)n\omega}. \quad (5.11)$$

By symmetry, pairs in subclasses (iia) and (iib) have equivalent PDFs, i.e., $g^{(iib)}(\omega) = g^{(iia)}(\omega)$, which implies

$$g^{(iib)}(\omega) = \int_0^\omega n [\xi_v e^{-nv \cup v'}]_{v'=\omega} dv = e^{-n\omega} - e^{(\zeta-2)n\omega}. \quad (5.12)$$

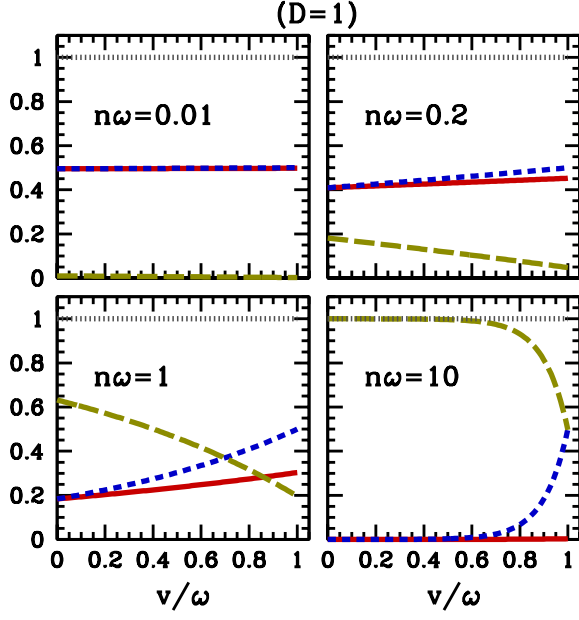


FIG. 7: (Color online) Contributions due to (ii), (iii) and (iv) pair configurations (solid, short dashed and long dashed lines, respectively) to the CPDF $g_v(\omega)$ as a function of v , for one dimensional Poisson ensembles and different distances as measured by ω (values $n\omega$ indicated on the plots). The total CPDF is shown by the dotted line.

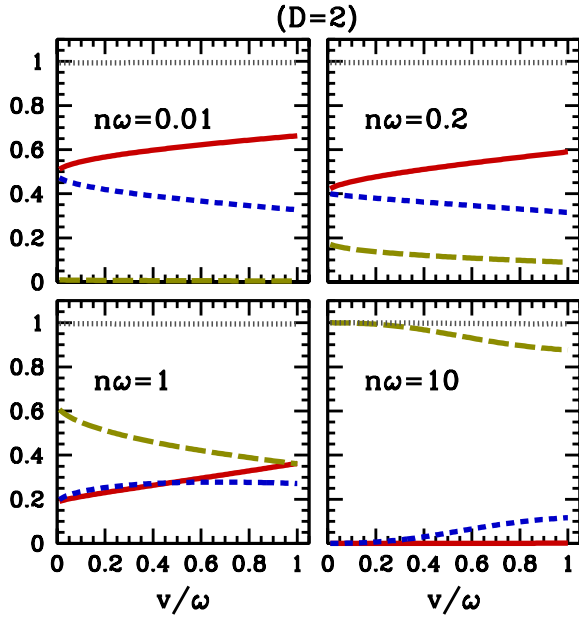


FIG. 8: (Color online) Same as Fig. 7, for $D = 2$.

A similar analysis applies to pairs in classes (iii) and (iv) but their contributions to $g_v(\omega)$ and $g(\omega)$ cannot be determined analytically except for $D = 1$ and $D = \infty$. In general, these functions are expressed as integral forms,

$$g_v^{(iii)}(\omega) = \int_0^\omega \eta_{vv'} e^{-nC_{v'}} dv' \Theta(\omega - v), \quad (5.13)$$

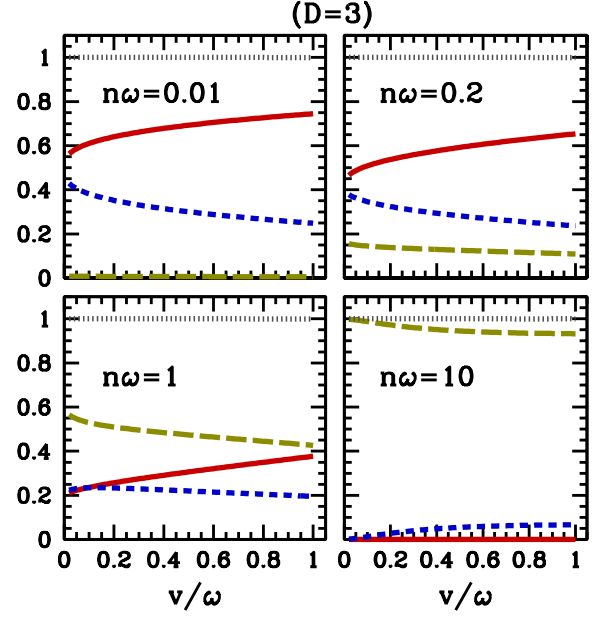


FIG. 9: (Color online) Same as Fig. 7, for $D = 3$.

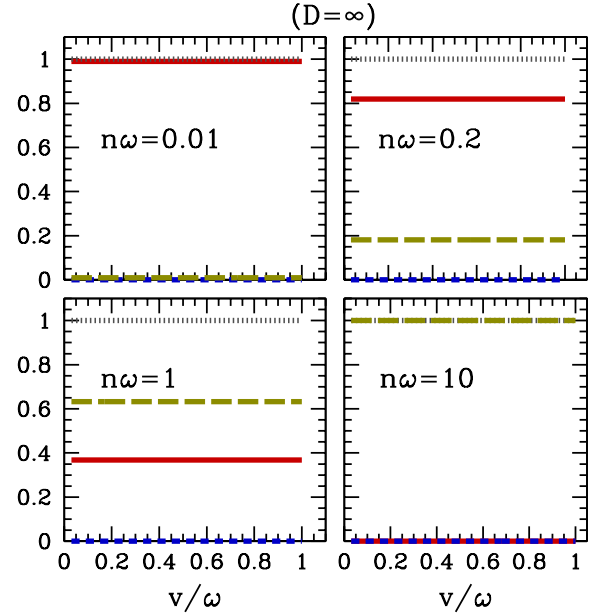


FIG. 10: (Color online) Same as Fig. 7, for $D = \infty$.

$$g_v^{(iv)}(\omega) = n \int_0^\omega \xi_v \xi_{v'} e^{-nC_{v'}} dv' \Theta(\omega - v), \quad (5.14)$$

$$g^{(iii)}(\omega) = n \int_0^\omega \int_0^\omega \eta_{vv'} e^{-nv \cup v'} dv' dv, \quad (5.15)$$

$$g^{(iv)}(\omega) = n^2 \int_0^\omega \int_0^\omega \xi_v \xi_{v'} e^{-nv \cup v'} dv' dv. \quad (5.16)$$

Again, by virtue of (2.7), the Heaviside term in (5.1)

comes from (5.9), (5.13) and (5.14), therefore

$$g_v^{(iii)}(\omega) + g_v^{(iv)}(\omega) = [1 - (\xi_v e^{-nC_{v'}})_{v'=\omega}] \Theta(\omega - v). \quad (5.17)$$

which implies

$$\int_0^\omega (\eta_{vv'} + n\xi_v \xi_{v'}) e^{-nC_{v'}} dv' = 1 - [\xi_v e^{-nC_{v'}}]_{v'=\omega}. \quad (5.18)$$

Similarly, with (5.12) and (5.17) we obtain

$$g^{(iii)}(\omega) + g^{(iv)}(\omega) = 1 - 2e^{-n\omega} + e^{(\zeta-2)n\omega}. \quad (5.19)$$

Explicit mathematical formulas for $g_v^{(\nu)}(\omega)$ and $g^{(\nu)}(\omega)$ functions at $D = 1$ and $D = \infty$ have been collected in Appendixes B and C.

The explicit expression for $g^{(i)}(\omega)$ at $D = 3$ [as given by Eq. (5.6)] was previously obtained by Larsen & Stratt [29]. To the best of our knowledge, all other results derived here are new.

B. Discussion

Figures 7, 8, 9 and 10 depict the partial probability densities $g_v^{(iib)}(\omega)$ (solid lines), $g_v^{(iii)}(\omega)$ (dashed lines) and $g_v^{(iv)}(\omega)$ (long dashed lines) as functions of the AV v ($0 \leq v < \omega$), for different volume ω and dimensions D . These evaluations come from Eqs. (5.9), (5.13), and (5.14). It is worth to notice that the sum of these three contributions gives the unity (dotted lines in the figures), which is actually the value of the total CPDF $g_v(\omega)$ for $v < \omega$ [Eq. (5.1)].

At finite dimension and short pair separations ($n\omega \ll 1$), the CPDF $g_v(\omega)$ is almost entirely composed of contributions due to pairs in classes (iib) and (iii), i.e., the reference point with AV v is the nearest neighbor of the other point at ω or both have a shared nearest neighbor. In the one dimensional system (Fig. 7), shared neighbor configurations (short dashed lines) are somewhat more likely than those in class (iib), while for $D > 1$ the major contribution arises from pair of class (iib) (solid lines, Figs. 8 and 9). Pairs sharing the nearest neighbor becomes highly unlikely at high space dimensionalities for any pair separation (Fig. 10). As expected, class (iv) (long dashed lines) is the dominant pair configuration at any D for great distances ($n\omega > 1$) from the reference point.

At finite dimension, as the available volume v of the reference point increases with fixed ω , the surface fraction ξ_v in Eq. (5.9) increases and the exclusion volume $C_{v'=\omega}$ decreases. Consequently, the probability of finding pairs at class (iib) increases monotonically with v . On the contrary, the chances of finding four-point configurations (pairs at class iv) reduce with increasing v (or decreasing ω) because the surface fraction $\xi_{v'}$ at the integrand of Eq. (5.14) takes on average lower values (which are not fully compensated by the increasing of the other terms in

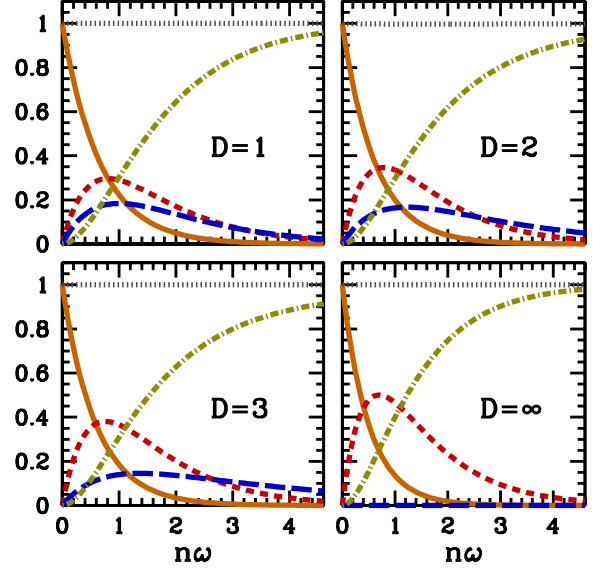


FIG. 11: (Color online) Contributions $g^{(\nu)}(\omega)$ due to $\nu = i, ii, iii$ and iv pair configurations (solid, short dashed, long dashed and point-dashed lines, respectively) to the PDF $g(\omega)$ vs the volume ω , for Poisson ensembles at dimensions $D = 1, 2, 3$ and ∞ . The total PDF is shown by a dotted line.

the integrand). The higher the Euclidean space dimensionality, the weaker the v dependence of the geometrical quantities ($\xi_v, \eta_{vv'}, C_{v'}$), and the partial probability densities $g_v^{(\nu)}(\omega)$ analyzed here become independent of v at the limit $D \rightarrow \infty$ (Fig. 10).

C. Relative importance of the different contributions to the PDF $g(\omega) = 1$

Figure 11 illustrates the behavior of the partial probability densities $g^{(\nu)}(\omega)$ given by Eqs. (5.6), (5.11), (5.12), (5.15) and (5.16). Note that $g^{(ii)}(\omega)$ is given by the sum of (5.11) and (5.12). The term $g^{(i)}(\omega)$ dominates the regime of low volume ($n\omega \ll 1$) at any D , i.e., most points with a first neighbor at very short distance (lower than the mean separation between points in the ensemble) form pairs of mutual nearest neighbors. At intermediate distances from a reference point (which correspond to $n\omega \approx 1$), there is a relatively narrow ω range where pairs in class (ii) are the main contribution to $g(\omega)$ for any D . As the distance from the reference point increases ($n\omega > 1$), pairs in class (iv) become the dominant contribution to $g(\omega)$. Indeed, $g^{(iv)}(\omega)$ is a monotonically increasing function of ω and tends asymptotically to unity, while the remaining contributions go to zero for ω large enough. The term $g^{(iii)}(\omega)$ corresponding to pairs with the shared nearest neighbor is never dominant and has a maximum contribution of 18.39%, 16.72% and 14.54% at $n\omega = 1, 1.226$ and 1.370 for $D = 1, 2$ and 3 , re-

TABLE II: Average fractions of pairs in various classes

D	α	ζ	$f^{(i)}$	$f^{(iia)} = f^{(iib)}$	$f^{(iii)}$	$f^{(iii)*}$
1	2	1/2	0.667	0.333	0.500	0.50
2	π	$\frac{4\pi-3^{3/2}}{6\pi}$	0.622	0.378	0.618	0.63
3	$4\pi/3$	$5/16$	0.593	0.407	0.709	0.71
∞	0	0	0.500	0.500	-	1.00

* Values listed in Ref. [58]

spectively. This maximum value gradually decreases and shifts to larger ω with increasing dimension D . The converse behavior is followed by $g^{(ii)}(\omega)$. Indeed, the maximum probability for the occurrence of pairs where one and only one of the two points is the nearest neighbor of the other occurs at $n\omega = 0.811$ (29.63%), 0.781 (34.67%), 0.761 (38.06%), and 0.694 (50%) for $D = 1, 2, 3$ and ∞ .

D. Pair fractions and mean separations

Finally we mention that one can use $g_{vv'}(\omega)$ to obtain other useful measures of the structure of Poisson ensembles or many-body systems in general. For examples, the fraction $f^{(\nu)}$ of points in classes $\nu = i, ii$ and iii , averaged over the whole ensemble, and the mean pair separation $\langle r \rangle^{(\nu)}$ in each class. They are defined as

$$f^{(\nu)} = \int_0^\infty n g^{(\nu)}(\omega) d\omega, \quad (5.20)$$

and

$$\langle r \rangle^{(\nu)} = \frac{1}{f^{(\nu)}} \int_0^\infty nr(\omega) g^{(\nu)}(\omega) d\omega, \quad (5.21)$$

with $r(\omega) = (\omega/\alpha)^{1/D}$. Results for pairs in classes (i) and (ii) at Poisson ensembles are found analytically using Eqs. (5.6), (5.11) and (5.12). Thus

$$f^{(i)} = \frac{1}{2 - \zeta}, \quad (5.22)$$

$$f^{(iia)} = f^{(iib)} = \frac{1 - \zeta}{2 - \zeta}, \quad (5.23)$$

$$\langle r \rangle^{(i)} = \frac{\Gamma(1 + \frac{1}{D})}{[n\alpha(2 - \zeta)]^{1/D}}, \quad (5.24)$$

$$\langle r \rangle^{(ii)} = \frac{\Gamma(1 + \frac{1}{D}) [(2 - \zeta)^{1+1/D} - 1]}{[n\alpha(2 - \zeta)]^{1/D} (1 - \zeta)}. \quad (5.25)$$

Notice that the nearest neighbor of any point is either mutual or non mutual one and therefore $f^{(i)} + f^{(iia)} = 1$. Mean values $\langle \omega \rangle^{(\nu)}$ can be also computed in similar form to $\langle r \rangle^{(\nu)}$,

$$\langle \omega \rangle^{(i)} = \frac{1}{n(2 - \zeta)}, \quad \langle \omega \rangle^{(ii)} = \frac{1}{n} + \langle \omega \rangle^{(i)}. \quad (5.26)$$

TABLE III: Mean ω -volumes and average distances between points of pairs in classes (i), (ii) and (iii). $\langle r \rangle$ and $\langle \omega \rangle$ are expressed in units of mean distance between points $n^{-1/D}$ and mean volume per point n^{-1} , respectively.

D	$\langle r \rangle^{(i)}$	$\langle r \rangle^{(ii)}$	$\langle r \rangle^{(iii)}$	$\langle \omega \rangle^{(i)}$	$\langle \omega \rangle^{(ii)}$	$\langle \omega \rangle^{(iii)}$
1	0.333	0.833	1.000	0.667	1.667	2.000
2	0.394	0.674	0.880	0.622	1.622	2.797
3	0.466	0.683	0.909	0.593	1.593	3.961

Clearly, results based on the volume ω are more concise than those upon the distance r .

The fraction $f^{(i)}$ of mutual nearest neighbors at Poisson ensembles was initially studied by Clark [55], although the exact evaluation [equivalent to that given by Eq. (5.22)] was obtained by Dacey [56] and Cox [57]. The fraction $f^{(iii)}$ of pairs sharing the nearest neighbor has also been computed by Schilling [58]. All these authors have used techniques different from that adopted in the present work, which are based on conditional pair distribution functions. Our evaluations of $f^{(\nu)}$, $\langle r \rangle^{(\nu)}$ and $\langle \omega \rangle^{(\nu)}$, together with values of the parameter α and the overlap volume ζ are listed in Tables II and III. Results corresponding to pairs in class (iii) were evaluated by numerical integration of (5.20) and (5.21). The fractions $f^{(iii)}$ computed here are in agreement with those obtained by Schilling [58] (see Table II). Interesting enough, Schilling showed that $f^{(iii)}$ tends to unity as $D \rightarrow \infty$. This implies that whereas $g_{vv'}^{(iii)}(\omega)$ tends to zero everywhere (see Section IV A) with $D \rightarrow \infty$, its integral over ω [Eq. (5.20)] converges to unity.

VI. CONCLUSIONS

A new mathematical descriptor of spatial structures in many-body systems have been proposed. Specifically, we have introduced a two-point distribution function, denoted by $g_{vv'}(\omega)$ and defined by Eq. (2.5), which describes the probability density of finding pairs of objects with each object having a nearest neighbor at a certain distance. For simplicity in the mathematical framework, distances between objects have been substituted by spherical volumes whose radii denote the separation between two objects of a pair (volume ω), and between each object and its nearest neighbor (volumes v and v').

The conditional pair distribution function (CPDF) $g_{vv'}(\omega)$ reveals a richer structural information than that provided by the conventional PDF $g(\omega)$. Indeed, the volumes v and v' introduce correlations in the CPDF which are not implicit in $g(\omega)$. Moreover, nearest neighbor information from v and v' let us to identify four types of pairs (mutual nearest neighbors and neighbor sharing pairs, among others), which provide a considerable amount of information concerning the local microscopic density and spatial relationships in many-body systems.

General relations were established among $g_{vv'}(\omega)$, the standard PDF $g(\omega)$, and $g_v(\omega)$. The function $g_v(\omega)$, pre-

viously introduced in [33], is a CPDF in which the nearest neighbor information is only considered for one object of each pair. We have shown that, using appropriate many-body interaction potentials, $g_v(\omega)$ and $g_{vv'}(\omega)$ can be used to evaluate the total potential energy of a fluid, which reduces to that typically adopted in liquid theory with an averaged pairwise potential. It was shown also that the potential energy expression based on $g_{vv'}(\omega)$ is the correct one to be used in the so-called thermostatical space partition (TSP) formalism [33, 34].

We have studied the function $g_{vv'}(\omega)$ for Poisson ensembles and derived its exact expression in any space dimension. We have obtained explicit results for $g_{vv'}(\omega)$ at $D = 1, 2, 3, \infty$, and found simple close forms for both $D = 1$ and $D = \infty$. To our knowledge, all these results are new. Furthermore, functions $g_{vv'}(\omega)$, $g_v(\omega)$ and $g(\omega)$ corresponding to Poisson systems have been deconvoluted into contributions from the four pair classes. With the exception of the function $g^{(i)}(\omega)$ given in [29] for mutual nearest neighbors at $D = 3$, all the partial probability densities obtained in the present study are new. Our theoretical results should have interesting and practical applications in the study of neighborhood structures in a variety of areas, such as physical and biological sciences, and sociology. The extension of present evaluations to non-Poisson processes is open to future efforts.

Acknowledgments

The authors are indebted to Professor Andrés Santos for helpful suggestions and comments. This work has been supported by CONICET (Argentina) through Grant PIP 112-200801-01474.

Appendix A: Covolume of two shells

In this Appendix we give a brief derivation of the scaled overlap volume $\eta_{vv'}$ of shells δv and $\delta v'$ surrounding the available volumes v and v' [Eq. (4.20)]. This quantity is directly related to the shared neighbor configuration in pairs (v, v') . The shared nearest neighbor of a pair (v, v') must be located in the intersection of the outer edges of v and v' . For $D = 1$, this intersection corresponds to a single point in space, which yields the Dirac delta function at (4.20) with a prefactor 1/2 because the shared neighbor is located in one of the two sides of v . At $D = 2$, $\delta v \cap \delta v'$ is the overlap surface of two off-center circular rings with thickness δa and δb , as shown in Fig. 4. It is shown easily by simple geometry that

$$\delta v \cap \delta v' = \frac{2\delta a \delta b}{\sin(\theta + \phi)}, \quad (D = 2), \quad (\text{A1})$$

where θ and ϕ are defined in Fig. 4 and expressed by Eqs (4.16) and (4.17). In the case $D = 3$, $\delta v \cap \delta v'$ is the overlap volume of two spherical shells with internal radii a and b , thickness δa and δb , and centers separated

a distance r . This intersection volume is a torus with section area $\delta a \delta b / \sin(\theta + \phi)$ and perimeter $2\pi R$, where θ and ϕ are defined as before and $R = a \sin \theta = b \sin \phi$. Therefore, we can write

$$\delta v \cap \delta v' = \frac{2\pi a \sin \theta \delta a \delta b}{\sin(\theta + \phi)}, \quad (D = 3). \quad (\text{A2})$$

Equation (4.20) at $D = 2$ and $D = 3$ results from (4.10), (A1) and (A2), once the radii (a and b) and thickness (δa and δb) are written in terms of $v = \alpha a^D$, $v' = \alpha b^D$, $\delta v = D\alpha a^{D-1}\delta a$ and $\delta v' = D\alpha b^{D-1}\delta b$, with α given by (2.1).

Appendix B: Partial probability densities at $D = 1$

For one-dimensional Poisson ensembles ($D = 1$), Eqs. (4.21), (5.3), and (5.4) yield

$$g_v^{(i)}(\omega) = \frac{1}{n} e^{-nv/2} \delta(\omega - v), \quad (\text{B1})$$

$$g_v^{(iia)}(\omega) = \frac{1}{n} \left(1 - e^{-nv/2}\right) \delta(\omega - v), \quad (\text{B2})$$

$$g_v^{(iib)}(\omega) = \frac{1}{2} e^{-n\omega + nv/2} \Theta(\omega - v), \quad (\text{B3})$$

$$g_v^{(iii)}(\omega) = \frac{1}{2} e^{-n(\omega - v)} \Theta(\omega - v), \quad (\text{B4})$$

$$g_v^{(iv)}(\omega) = \left[1 - \frac{1}{2} \left(e^{-n(\omega - v)} + e^{-n\omega + nv/2}\right)\right] \Theta(\omega - v), \quad (\text{B5})$$

and

$$g^{(i)}(\omega) = e^{-3n\omega/2}, \quad (\text{B6})$$

$$g^{(iia)}(\omega) = g^{(iib)}(\omega) = e^{-n\omega} - e^{-3n\omega/2}, \quad (\text{B7})$$

$$g^{(iii)}(\omega) = \frac{n\omega}{2} e^{-n\omega}, \quad (\text{B8})$$

$$g^{(iv)}(\omega) = 1 - \frac{n\omega}{2} e^{-n\omega} - 2e^{-n\omega} + e^{-3n\omega/2}, \quad (\text{B9})$$

Clearly, the sum of terms $g_v^{(\nu)}(\omega)$ and $g^{(\nu)}(\omega)$ over all pair classes ($\nu = i, iia, iib, iii$ and iv) let us recover the exact expressions for $g_v(\omega)$ and $g(\omega)$, Eqs. (5.1) and (5.2), respectively.

Appendix C: Partial probability densities at $D = \infty$

For Poisson ensembles at infinity dimensions, Eqs. (4.21), (5.3), and (5.4) yield

$$g_v^{(i)}(\omega) = \frac{1}{n} e^{-nv} \delta(\omega - v), \quad (\text{C1})$$

$$g_v^{(iia)}(\omega) = \frac{1}{n} (1 - e^{-nv}) \delta(\omega - v), \quad (\text{C2})$$

$$g_v^{(iib)}(\omega) = e^{-n\omega} \Theta(\omega - v), \quad (\text{C3})$$

$$g_v^{(iii)}(\omega) = 0, \quad (\text{C4})$$

$$g_v^{(iv)}(\omega) = (1 - e^{-n\omega}) \Theta(\omega - v), \quad (\text{C5})$$

and

$$g^{(i)}(\omega) = e^{-2n\omega}, \quad (\text{C6})$$

$$g^{(iia)}(\omega) = g^{(iib)}(\omega) = e^{-n\omega} - e^{-2n\omega}, \quad (\text{C7})$$

$$g^{(iii)}(\omega) = 0, \quad (\text{C8})$$

$$g^{(iv)}(\omega) = 1 - 2e^{-n\omega} + e^{-2n\omega}. \quad (\text{C9})$$

As in the case $D = 1$ (Appendix B), Eqs. (5.1) and (5.2) are recovered from (C1-C5) and (C6-C9), respectively.

Appendix D: Attractive hard spheres in the TSP approach

The model of attractive hard spheres can be used to check the role played by the CPDF in the evaluation of the potential energy contribution within the TSP approach. We consider a pair interaction potential which consists of a hard core repulsion together with an attractive square well,

$$u(\omega) = \begin{cases} \infty, & \omega \leq a, \\ -\epsilon, & a < \omega < a + \xi, \\ 0, & \omega \geq a + \xi, \end{cases} \quad (\text{D1})$$

with a , ξ and ϵ constants. For the present purpose, we may use the expression of $g_v(\omega)$ given in [33] [eq. (41)] at the low density limit, i.e.,

$$g_v(\omega) = \frac{1}{n} \delta(\omega - v - a^*) + \Theta(\omega - v - a^*), \quad (\text{D2})$$

where $\Theta(x)$ is the Heaviside step function and $a^* = a/2$ is a reduction of the AV of hard particles in the limit of low density. Thus, with (D1) into Eq. (3.10) we obtain

$$\phi_v = \begin{cases} +\infty, & v \leq b, \\ -\epsilon [1 + n(b + \xi - v)], & b < v < b + \xi, \\ 0, & \omega \geq b + \xi, \end{cases} \quad (\text{D3})$$

where $b = a - a^*$. With help of Eqs. (3.7) and (3.8) in the thermodynamic limit ($N, V \rightarrow \infty$ with $N/V = n$ constant) one finds

$$n_v = \frac{n\beta\gamma}{B} e^{\beta[\gamma(v-b)+\phi_v]} \quad (\text{D4})$$

and

$$\beta\gamma = n \frac{B}{C}, \quad (\text{D5})$$

with

$$B = e^{-\beta\gamma\xi} + \beta\gamma e^{\beta\epsilon(1+n\xi)} \left[\frac{1 - e^{-\beta(\gamma+n\epsilon)\xi}}{\beta(\gamma+n\epsilon)} \right] \quad (\text{D6})$$

and

$$C = [1 + \beta\gamma(b + \xi)] e^{\beta\gamma\xi} + \left[\frac{\beta\gamma}{\beta(\gamma+n\epsilon)} \right]^2 e^{\beta\epsilon(1+n\xi)} \\ \times \{1 + \beta(\gamma+n\epsilon)b - [1 + \beta(\gamma+n\epsilon)(b + \xi)] \\ \times e^{-\beta(\gamma+n\epsilon)\xi}\} \quad (\text{D7})$$

The contact value $g(\omega = a^+)$ of the PDF given in Eq. (3.13) is directly obtained from Eq. (2.6).

-
- [1] P. J. Clark and F. C. Evans, *Ecology* **35**, 445 (1954).
[2] F. D. K. Roberts, *Biometrika* **56**, 401 (1969).
[3] W. H. Burt, *Journal of Mammalogy* **24**, 346 (1943).
[4] E. J. Temeles, *Anim. Behav.* **47**, 339 (1994).
[5] H. J. Schenk, R. M. Callaway and B. E. Mahall, *Adv. Ecol. Res.* **28**, 145 (1999).
[6] P. J. Clark and F. C. Evans, *Science* **121**, 397 (1955).
[7] J. L. Brown and G. H. Orians, *Ann. Rev. Ecology and Systematics* **1**, 239 (1970).
[8] S. Getzin, T. Wiegand, K. Wiegand and F. He, *J. Ecology* **96**, 807 (2008).
[9] R. Cowana and N. Jonard, *J. of Econ. Dynam. Control* **28**, 1557 (2004).
[10] N. Miller and J. Dollard, *Social Learning and Imitation* (Yale University Press, 1941).
[11] A. Bandura, *Social Learning Theory* (General Learning Press, 1977).
[12] V. Bala and S. Goyal, *Rev. Econ. Stud.* **65**, 595 (1998).
[13] D. A. Moore and T. E. Carpenter, *Epidem. Rev.* **21**, 143 (1999).
[14] R. Balescu, *Equilibrium and Nonequilibrium Statistical Mechanics* (Wiley, Toronto, 1975).
[15] J.-P. Hansen and I. R. McDonald, *Theory of Simple Liquids*, 3rd ed. (Academic Press, London, 2006).
[16] R. L. Liboff, *Phys. Rev. A* **39**, 4098 (1989).
[17] P. J. E. Peebles, *Principles of Physical Cosmology* (Princeton University Press, Princeton, NJ, 1993).
[18] R. L. McGreevy, A. Baranyai and I. Ruff, *Phys. Chem. Liq.* **16**, 47 (1986).
[19] U. F. Edgal, *J. Chem. Phys.* **94**, 8191 (1991).
[20] S. Mazur, *J. Chem. Phys.* **97**, 9267 (1992).
[21] T. Keyes, *J. Chem. Phys.* **110**, 1097 (1999).
[22] B. Bhattacharjee, *Phys. Rev. E* **67**, 041208 (2003).
[23] P. Hertz, *Math. Ann.* **67** 387 (1909).

- [24] H. Reiss and R. V. Casberg, *J. Chem. Phys.* **61**, 1107 (1974).
- [25] J. R. Macdonald, *Mol. Phys.* **44**, 1043 (1981).
- [26] S. Torquato, B. Lu and J. Rubinstein, *Phys. Rev. A* **41**, 2059 (1990).
- [27] S. Chandrasekhar, *Rev. Mod. Phys.* **15**, 1 (1943).
- [28] H. Margeneau and M. Lewis, *Rev. Mod. Phys.* **31**, 569 (1959).
- [29] R. E. Larsen and R. M. Stratt, *Chem. Phys. Lett.* **297**, 211 (1998).
- [30] T-M. Wu, S. L. Chang and K. H. Tsai, *J. Chem. Phys.* **122**, 204501 (2005).
- [31] A. C. Pan, J. P. Garrahan and D. Chandler, *ChemPhysChem* **6**, 1783 (2005).
- [32] Y. Jiao, F. H. Stillinger and S. Torquato, *Phys. Rev. E* **81**, 011105 (2010).
- [33] R. D. Rohrmann, *Physica A* **347**, 221 (2005).
- [34] R. D. Rohrmann and J. Zorec, *Phys. Rev. E* **74**, 041120 (2006).
- [35] D. Hummer and D. Mihalas, *Astrophys. J.* **331**, 794 (1988).
- [36] R. D. Rohrmann, A. M. Serenelli, L. G. Althaus and O. G. Benvenuto, *Mon. Not. R. Astron. Soc.* **335**, 499 (2002).
- [37] H. C. Graboske, Jr, D. J. Harwood and F. J. Rogers, *Phys. Rev.* **186**, 210 (1969).
- [38] J. Frenkel, *Kinetic Theory of Liquids* (Dover, New York, 1955).
- [39] E. N. Gilbert, *Ann. Math. Statist.* **33**, 958 (1962).
- [40] P. J. Diggle, *Statistical Analysis of Spatial Point Patterns*, 2nd ed. (Arnold, London, 2003)
- [41] J. Bahcall and R. M. Soneira, *Astrophys. J.* **246**, 122 (1981)
- [42] M. Gómez, L. Hartmann, S. J. Kenyon, and R. Hewett, *Astronom. J.* **105**, 1927 (1993).
- [43] M. Longhitano and B. Binggeli, *Astron. and Astrophys.* **509**, A46 (2010)
- [44] F. H. Ree and C. F. Bender, *Phys. Rev. Lett.* **32**, 85 (1974).
- [45] M. Ross, F. H. Ree and D. A. Young, *J. Chem. Phys.* **79**, 1487 (1983).
- [46] R. J. Hemley, H. K. Mao, L. W. Finger, A. P. Jephcoat, R. M. Hazen and C. S. Zha, *Phys. Rev. B* **42**, 6458 (1990).
- [47] J. M. Aparicio and G. Chabrier, *Phys. Rev. E* **50**, 4948 (1994).
- [48] P. Wind and I. Roeggen, *Chem. Phys.* **211**, 179 (1996).
- [49] P. Soldán, M. T. Cvitas and J. M. Hutson, *Phys. Rev. A* **67**, 054702 (2003).
- [50] C. Russ, M. Brunner, C. Bechinger and H. H. von Grünberg, *Europhys. Lett.* **69**, 468 (2005)
- [51] P. Bergeron, M. T. Ruiz, and S. K. Leggett, *Astrophys. J., Suppl. Ser.* **108**, 339 (1997).
- [52] J. Largo, J. R. Solana, S. B. Yuste and A. Santos, *J. Chem. Phys.* **122**, 084510 (2005).
- [53] Y. Tang and B.C.Y. Lu, *J. Chem. Phys.* **100**, 6665 (1994).
- [54] At odd-dimensional spaces, $v \cap v'$ may be calculated from Eqs. (B10) and (B16) of R. D. Rohrmann and A. Santos, *Phys. Rev. E* **83**, 011201 (2011).
- [55] P. J. Clark, *Science* **123**, 373 (1956).
- [56] M. F. Dacey, *Geographical Analysis* **1**, 385 (1969).
- [57] T. F. Cox, *Biometrics* **37**, 367 (1981).
- [58] M. F. Schilling, *Adv. Appl. Prob.* **18**, 388 (1986).